Fibers and Polymers 2016, Vol.17, No.12, 2131-2142
DOI 10.1007/s12221-016-6253-x

ISSN 1229-9197 (print version)
ISSN 1875-0052 (electronic version)

Flexural and Hydrothermal Aging Behavior of Silk Fabric/Glass Mat Reinforced Hybrid Composites

Defang Zhao[1], Yuying Dong[1], Jing Xu[1], Yuqiu Yang[1,2]*, Kiyoshi Fujiwara[3], Erika Suzuki[4], Takashi Furukawa[5], Yuka Takai[6], and Hiroyuki Hamada[7]

[1]*College of Textiles, Donghua University, Shanghai 201620, P.R. China*
[2]*Key Laboratory of Textile Science & Technology, Ministry of Education, Shanghai 201620, P.R. China*
[3]*Mazda Motor Corporation, Hiroshima 7308670, Japan*
[4]*Toyugiken Co., Ltd., Kanagawa 2500101, Japan*
[5]*HISHIKEN Co., Ltd., Kyoto 6048165, Japan*
[6]*Department of Information Systems Engineering, Osaka Sangyo University, Osaka 5740013, Japan*
[7]*Advanced Fibro-Science, Kyoto Institute of Technology, Kyoto 6068585, Japan*
(Received March 6, 2016; Revised October 10, 2016; Accepted October 10, 2016)

Abstract: Recycled natural materials such as silk fabric have attracted more and more public attention over the past few years. In this research, unsaturated polyester resin was used as matrix, glass mat and silk fabric were employed as reinforcement to fabricate the laminated hybrid composites by hand lay-up method. Three-point flexural quasi-static and load-controlled low cycle bending fatigue (LCBF) tests at 55 %, 70 % and 85 % pre-set load levels were performed. The composite specimens were also subjected to hot water immersion treatment at 80 °C for different durations. The effects of the immersion treatment on the bending and impact fracture characteristics were investigated. The results showed that higher flexural modulus and strength were obtained when silk fabric layer was stacked at the middle layer. It seems that the anti-fatigue property was improved by the inclusion of silk fabric reinforced in glass mat hybrid composites. In the water immersion experiments, both the flexural properties and impact properties were improved initially until reaching the maximum and then decreased continuously with further increase in exposure time. These seemingly contradictory behaviors are due to relaxation of the internal stress, swelling of the silk fibers and the weakening of fiber/matrix interface.

Keywords: Glass mat, Silk fabric, Hybrid laminated sequence, Low cycle bending fatigue (LCBF), Hydrothermal degradation

Introduction

Fiber reinforced polymer composites (FRPs) have been increasingly used in many areas during the past decades due to their attractive properties, such as light weight, corrosion resistance, and easy to design with low cost.

A key problem regarding the engineering diffusion of FRPs is the study of their resistance to cyclic stresses. FRPs offer substantial improvements over metals not only for the high specific stiffness and strength, but also for their resistance to fatigue [1].

Fatigue in a material occurs when it is subjected to repetitive, intermittent stresses. Many of these materials usually have a limiting stress below which fatigue failure does not occur. Failure of FRPs under fatigue loading is more complicated than for metals because of anisotropic characteristics in strength and stiffness. In fact, the heterogeneous and anisotropic nature of FRPs leads to the formation of different stress levels within the material so that the fracture process includes various combinations of damage modes such as matrix cracking, fiber breakage, delamination, debonding, and ply failure. Fatigue failure in fibrous composites proceeds in general by the accumulation of damage throughout the material. Fracture eventually occurs through the propagation of damage at some cross-section of the material [2].

In many structural applications, repeated loading can cause failure of the material. Thus, there is a strong need to develop effective analysis and methodology for assessing the safety and reliability of using polymeric composites in these applications. The fatigue behavior of FRPs has been studied by many researchers.

Belingardi *et al.* [3] studied a hybrid glass-carbon fiber reinforced epoxy matrix composite, characterized by the presence of intraply biaxial glass-carbon laminae as well as biaxial glass laminae and biaxial carbon laminae, was considered for its bending fatigue behavior. Research showed that reduction in material strength and elastic modulus was found to depend on the level of fatigue loading. However, tThe reduction in stiffness did not exactly correlate with the reduction in strength.

From the research of Kulkarni and Mahfuz [4], fatigue crack growth of foam core sandwich beams loaded in flexure has been investigated. It was found that the first visible sign of damage initiation was a core-skin debond parallel to the beam axis. This debond propagated slowly along the top interface and eventually kinked into the core as shear crack and then grew in an unstable manner resulting in total specimen collapse. A fatigue model based on this crack growth has been developed and validated with experiments.

*Corresponding author: amy_yuqiu_yang@dhu.edu.cn

Couillard and Schwartz [5] conducted research on the bending fatigue behavior of unidirectional, continuous-carbon-fiber/epoxy composite strands. It was determined that the composite did undergo fatigue, the fatigue damage being manifested as a loss of bending resistance. At high strains, damage occurred through fiber breakage, matrix cracking, and interfacial shear failure. As the number of bending cycles increased, there was crack growth in the matrix along fiber interfaces. At the imposed radius of curvature and up to 10^6 cycles, the loss in bending moment followed an exponential decay.

The work of Xu *et al*. [6], mechanical properties of kenaf/UP, such as tensile properties and bending properties were investigated and discussed, as well as the low cycle fatigue (LCF) behavior. The results showed that for both un-notched and notched kenaf/UP, tensile strength decreased when the preset load was increased to 70 % and 85 %, and both can't survive from the LCF test of 30 cycles. On the other hand, bending results had shown similarity of tendency in low fatigue bending test as tensile results.

An extensive experimental program has been carried out by Nixon-Pearson *et al*. [7,8] to investigate and understand the sequence of damage development throughout the life of open-hole quasi-isotropic IM7/8552 carbon-fiber/epoxy laminates loaded in tension-tension fatigue. The obtained results show that the predicted damage process had a close match to that observed experimentally. Matrix cracking at the surface ply and initiation of matrix cracks in the subsequent plies lead to delamination through thickness, and ultimately to failure at the $45^{o}/0^{o}$ interface. When run at different severities the model could predict an S-N curve which had good agreement to tests.

Koricho *et al.* [9] carried experiments on bending fatigue behavior on twill E-glass/epoxy composite. The amount of stiffness reduction was observed to be a function of the magnitude of the fatigue loading applied to the specimen. Different levels of reduction on material strength and elastic modulus were found to depend on the level of fatigue loading.

The work of Van Paepegem and Degrieck [10] presents an investigation of the fatigue performance of plain woven glass/epoxy composite materials. Experiments show that these two specimens in two different configurations: $[\#0^{o}]_8$ and and $[\#45^{o}]_8$ had a quite different damage behavior and that the stiffness degradation followed a different path. A numerical model was presented which allows one to describe the degradation behaviour of the composite specimen during its fatigue life.

In marine applications, the FRPs are exposed to harsh and changing environments featuring a wide range of temperatures and "hot-wet" exposures, which accelerate decline in their mechanical and other properties [11,12]. And a variety of correlative experimental and theoretical researches have been done to discuss the impact of aging on the material performance.

Water uptake in FRPs is activated by three main mechanisms: water diffusion in glassy polymer matrices [13-15], water diffusion at fiber/matrix interfaces [16], and water uptake by mesoscale voids [16-18]; while diffusion into glass or carbon fibers is usually negligible. The latter two mechanisms, in particular, characterise FRPs, due to the presence of a mesoscopic free volume [16], which is mainly reached and filled by capillarity, and is responsible for a final relative water uptake higher than that absorbed by an equivalent weight of bulk matrix resin. The action of water in these fiber/matrix and matrix mesoscale voids can also provide the onset for further damage, and favour non-fickian diffusion behavior or pseudo-equilibrium stages with the progression of absorption [16-19].

Aging by water absorption in FRPs may then induce various effects: plasticization of the matrix, molecular degradation with breaking of the polymeric chains, swelling [20,21] and induced internal stresses, cracking/crazing due to both osmosis and change of water state, damage of matrix/fiber interface with debonding [22,23] phenomena. By their nature, all these matrix and fiber/matrix transformations are expected to have an influence on interlaminar delamination toughness. There is hence a special need to understand and predict how these effects may interfere with the interlaminar delamination behavior, which is typically quantified through the Strain Energy Release Rate (SERR), at both delamination onset (initiation) or stable growth (propagation) [24].

Undoubtedly, a better understanding on the effect of LCBF behavior and the moisture on the mechanical properties of the silk fabric/glass mat reinforced hybrid composites is essential for the applications of such hybrid composites. In this paper, we will report a study on the three-point bending and LCBF behavior, weight changes characteristics and the water absorption effect on the bending and impact properties of the hybrid composites. Optical and scanning electron microscopy observations were utilized to check the fractured surfaces of materials during LCBF and hydrothermal aging tests.

Experimental

Materials Preparation and Fabrication

Unsaturated polyester resin with no additives was used for matrix. Glass mat and silk fabric were employed as reinforcement. The silk fabric, which is a type of plain weave fabric, with the creases embossed on the surface of the fabric, produced using hard-twist yarn for weft yarn, as illustrated in Figure 1. Glass mat (Nitto Glass tex Co., Ltd.) with gram weight of 450 g/m^2 was made of continuous glass fiber bundles, cut into lengths of 50 mm. The chopped glass bundles are distributed in random directions, as depicted in Figure 2. These materials were used to fabricate hybrid

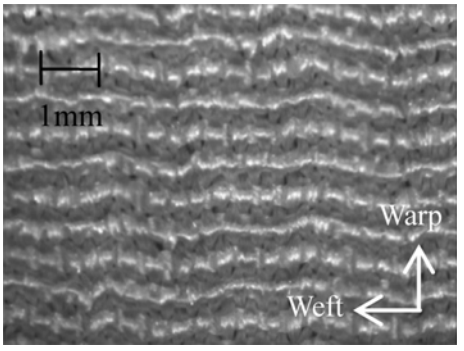

Figure 1. Photo of silk fabric.

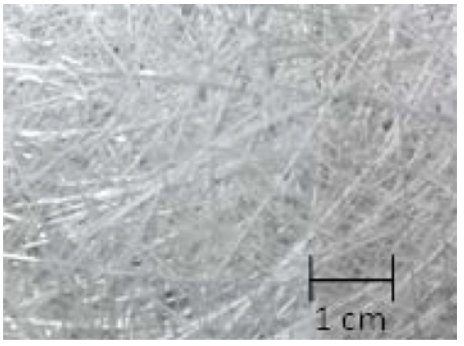

Figure 2. Photo of glass mat.

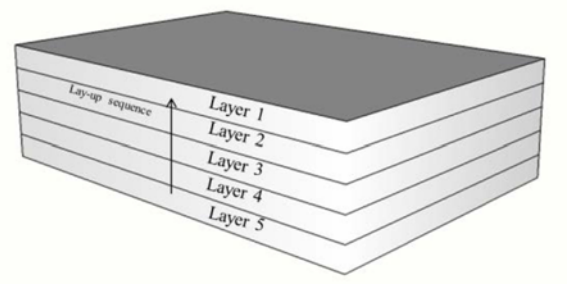

Figure 3. Diagram of lay-up sequence for hybrid composites and GFRP.

composites with the hand lay-up molding method. First, gel coating was layered on the innermost layer, on which a sheet of glass mat or silk fabric was layered according the stacking sequence. A sheet of gel coating was then layered on the outermost layer. It is important to ensure that bubbles are not trapped in between the fibers, thus, a steel roller was moved on the composite to remove trapped air. For glass mat reinforced plastics (GFRP), the material was fabricated in the same procedure without adding the silk fabric. Finally, the blocks of the composite pressed and naturally cured for 12 hours in ambient temperature, post cure was followed in an oven of 55 °C maintained 1 hour.

Schematic drawing of lay-up sequence for hybrid composites and GFRP is shown in Figure 3. Hybrid composites had a stacking sequence of four layers of glass mat and one layer of silk fabric, which was in the first, third, fifth layer, respectively. The volume fraction of glass fiber and silk fiber of hybrid composites was determined to be about 14.5 % and 2.4 %, respectively. While glass fiber volume fraction of GFRP was approximately 22.0 %.

Experiments Details

Three-point Bending

The composites were cut into rectangular samples with dimensions of 90 mm×15 mm×4.5 mm according to ASTM D 790-2003 flexural testing standard, i.e. three-point flexural technique was adopted. Static bending tests were conducted by QJ-212C with the span of 72 mm at a cross- head speed of 1 mm/min in ambient atmosphere at room temperature. At least three pieces of specimens were repeated. The camera system was employed to record the damage process of the specimens. According to the time, different damage state can be obtained from the video.

Low Cycle Bending Fatigue (LCBF)

In the low cycle bending fatigue (LCBF) evaluation, the cycle load was calculated and determined by the maximum value of load obtained from the quasi-static bending test. In addition, 30 cycles was performed by QJ-212C at a constant loading speed of 1 mm/min with the span of 72 mm when the load reached pre-set load, which were 55 %, 70 % and 85 % of the corresponding maximum load, respectively. In order to investigate the residual flexural properties after fatigue tests, static bending tests after fatigue tests were also conducted in the same environment as fatigue tests. Then, the final flexural properties after 30 cycles were compared with that of non-cycle, to see if there was any change effected by the LCBF test.

Izod Impact

Izod impact without notch was performed on the Impact tester, pendulum 5.5 J in accordance with ADTM D-256-2005. According to standards, the specimens were cut into 80 mm×10 mm×4.5 mm. Five specimens were tested to guarantee the results' accuracy.

Hydrothermal Aging

All the specimens were first dried under vacuum for 24 hours at 100 °C prior to immersion in distilled water baths at 80 °C. Predetermined aging intervals were consisted of 1 day, 10 days, 30 days and 90 days, respectively. So as to discuss the effect of hydrothermal aging, the weight change behaviors were recorded periodically with a 10^{-3} g precision balance. The water absorption characteristics of the composites were evaluated by two parameters: the percentage of apparent weight gain (WG), and the percentage of weight loss (WL), which are given by the following two equations:

$$WG = \frac{m_1 - m_0}{m_0} \times 100\% \quad (1)$$

$$WL = \frac{m_0 - m_2}{m_0} \times 100\% \quad (2)$$

where m_0, m_1 and m_2 are, the initial sample weight, the weight after immersion, and the weight of the immersed sample after drying during certain days at 80 °C under vacuum, respectively. Each dot on the weight change curves is a mean value of 8 samples. After soaking in distilled water baths for certain days, the dry specimens were carried out for bending and Izod impact test.

Results and Discussion

Bending Properties

Results of Three-point Bending Test

The flexural properties of hybrid composites 1-W, 3-W, 5-W and GFRP are displayed in Figure 4. It is observed that the flexural strength reached a maximum value of 150.7 MPa for hybrid specimen 3-W (i.e. silk fabric in the middle layer of hybrid composites, the length of specimen in the warping direction of silk fabric) followed by 136.1 MPa for 1-W and 141.4 MPa for 5-W. Observations on specimens 1-F, 3-F, and 5-F showed that the maximum flexural strength was noticed at around 144.5 MPa for hybrid specimen 3-F when the deflection reached about 4.9 mm. Thereafter, there was a sudden decline to a value.

Furthermore, the results presented in Figure 4 are summarized in Figures 5 and 6 showing the average of the flexural strength, flexural modulus and maximum deflection. As depicted in Figure 5, the maximum flexural modulus and strength were achieved in hybrid composites 3-W, that exhibited about respective 16.3 % and 8.1 % higher than the values of 1-W. In addition, the flexural deflection obtained for 3-W was approximately 16.1 % below than that of 1-W as shown in Figure 6. In fact, GFRP showed higher flexural properties than 3-W due to high fiber content. When referred to flexural properties of hybrid composites in the 0 ° and 90 ° directions, take the specimens 3-W and 3-F as examples, the results showed that both flexural modulus and strength of 3-W were similar to the values of 3-F and showed the respective value of 5.7 GPa and 144.2 MPa with a minimum deflection of 5.2 mm.

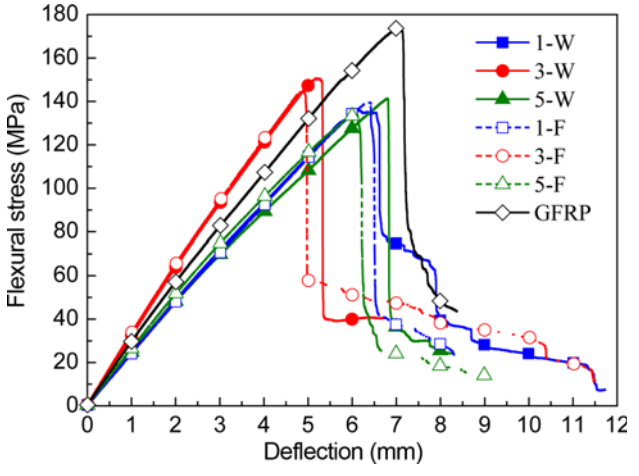

Figure 4. Typical flexural stress-deflection curves of hybrid composites and GFRP.

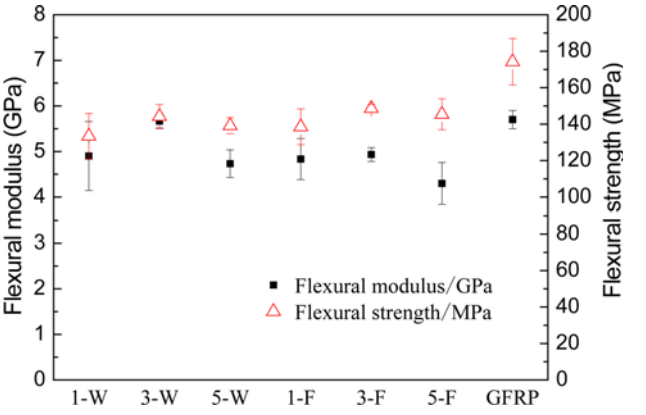

Figure 5. Comparison of flexural modulus and flexural strength.

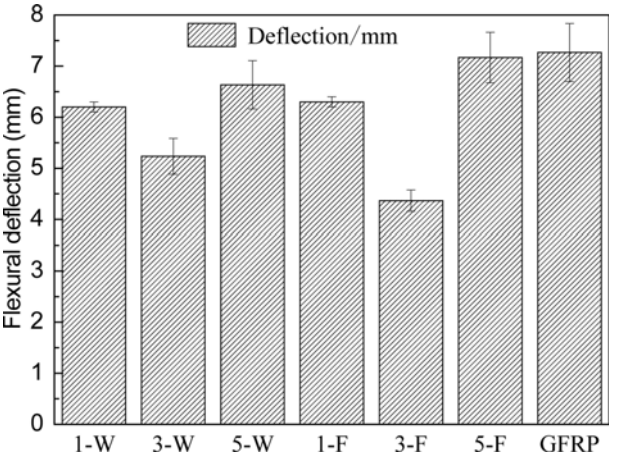

Figure 6. Comparison of flexural deflection.

It seems that hybrid composites 3-W exhibited better flexural properties compared to other two hybrid composites. On the other hand, the comparison of hybrid composites in the 0 ° and 90 ° directions showing in the Figures 5 and 6 are illustrating that the flexural properties in the 0 ° and 90 ° directions reported similar results, even though there was a dramatic difference existing in warp and filling direction of silk fabric.

Results of LCBF Test

The pre-set load for the LCBF test was set to be 55 %, 70 % and 85 % of the maximum bending load. The flexural modulus were recorded every three cycles, in order to see the tendency of the bending performance during the LCBF test. Additionally, the final flexural modulus and strength after the LCBF test were compared with normal bending and the decreasing ratio of flexural strength and modulus were employed to evaluate the effect of the LCBF test.

With respect to the flexural modulus, the summary during

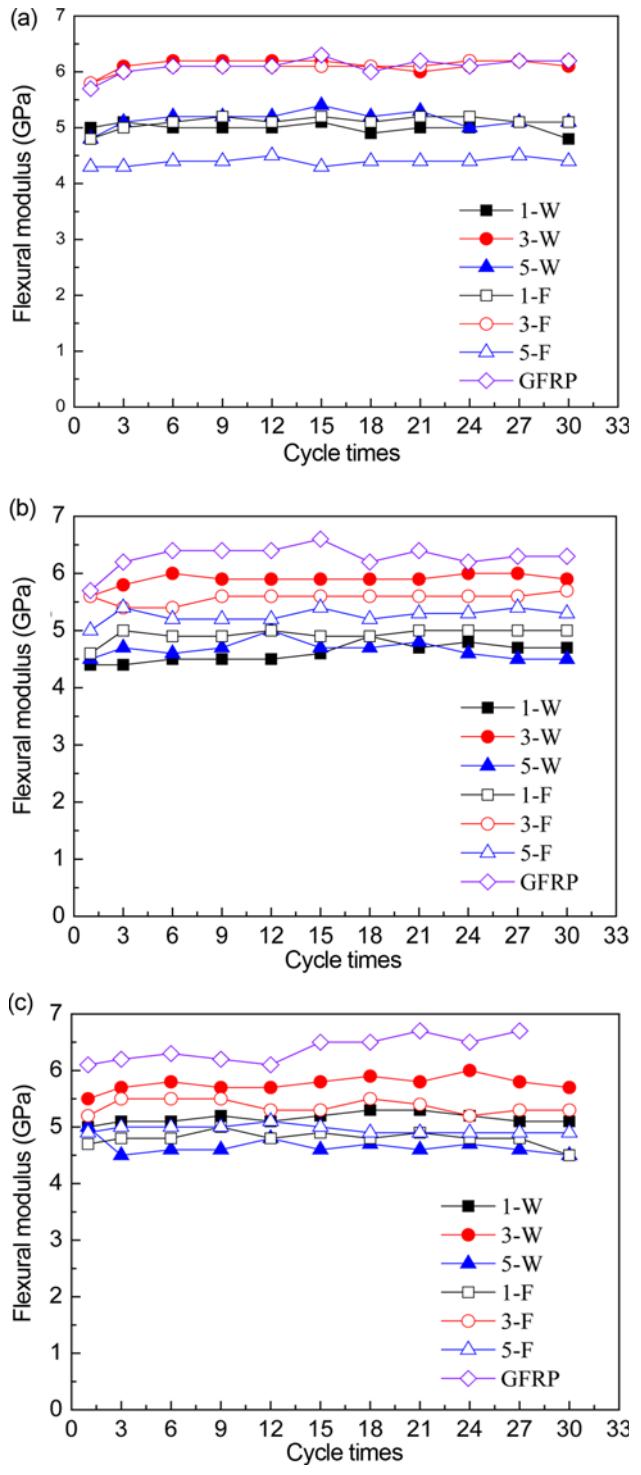

Figure 7. Flexural modulus during the LCBF test: (a) 55 % pre-set load LCBF, (b) 70 % pre-set load LCBF, and (c) 85 % pre-set load LCBF.

the 55 %, 70 % and 85 % LCBF test was shown in Figure 7, which was calculated every three times, and included flexural modulus from the final bending test. In the case of

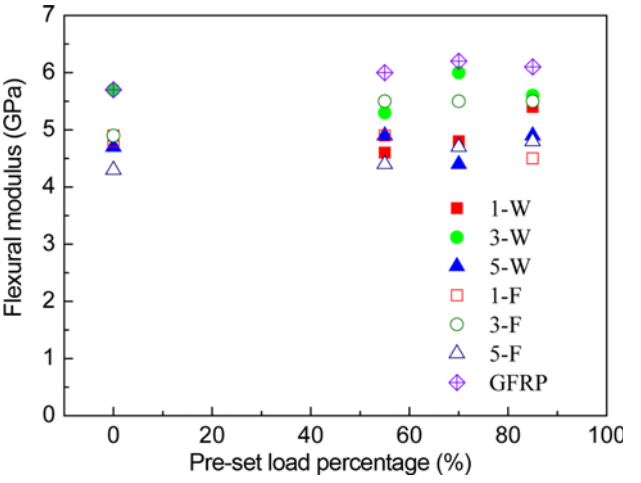

Figure 8. Comparison of flexural modulus between normal bending test and after 50 %, 70 %, and 85 % pre-set load LCBF.

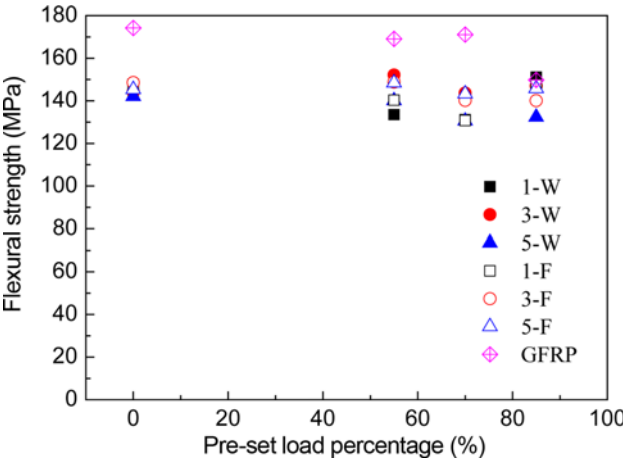

Figure 9. Comparison of flexural strength between normal bending test and after after 50 %, 70 %, and 85 % pre-set load LCBF.

1-F specimen at 85 % pre-set load, it can be seen from Figure 7(c) that, flexural modulus was around 4.8 GPa during the LCBF test, which hardly changed with a CV (coefficient of variation) value of 2.6 %. Additionally, it can be observed from Figure 7(c) that the fracture occurred on the specimen GFRP at the 27th cycle during the LCBF test, which was suggesting that they can't survive from 30 cycles test in the condition of 85 % pre-set load.

The final dates were compared in Figures 8 and 9. After 30 cycles fatigue test, three pre-set load levels (i.e. 55 %, 70 % and 85 %) LCBF made no difference on hybrid composites in both flexural modulus and strength. On the other hand, in the case of GFRP specimen, 85 % pre-set load LCBF resulted in strength decreasing by 14.0 % but the modulus barely changed.

Additionally, during the LCBF, flexural properties of

hybrid composites in the 0° and 90° directions showed no much variation at three pre-set load levels. In the case of 3-W and 3-F subjected to 70 % pre-set load LCBF, both the flexural modulus and strength barely changed with a changing rate below 6 % after LCBF test compared with normal results.

In summary, the flexural properties of hybrid composites were hardly affected by the 30 cycles LCBF test, while when referred to GFRP, flexural modulus also showed stable in LCBF test. Nevertheless, flexural strength did not changed much in the case of pre-set load 55 % and 70 % but degraded when the pre-set load enhanced to 85 % after the LCBF test. And GFRP were not able to survive from the LCBF test of 30 cycles when the pre-set load was 85 % of the maximum load. It seems that the inserted silk fabric can make a contribution to the anti-fatigue property of GFRP.

Fracture Mechanism

In order to gain insight into the damage mechanisms, digital camera was utilized to record whole damaging processes during normal bending and LCBF tests. After checking all experimental photographs and videos, it was displayed that crack initiated at the tension side and then progressively propagated through the thickness direction in both normal bending and LCBF specimens. And the fractural process was illustrated in Figure 10 (observing from the tension side of specimens), the generating flexural fracture could be seen at different stages under flexural loading. Initial cracks as showing white area can be seen clearly when the stress reached close to maximum stress, and then propagated through the specimen gradually until complete failure occurred.

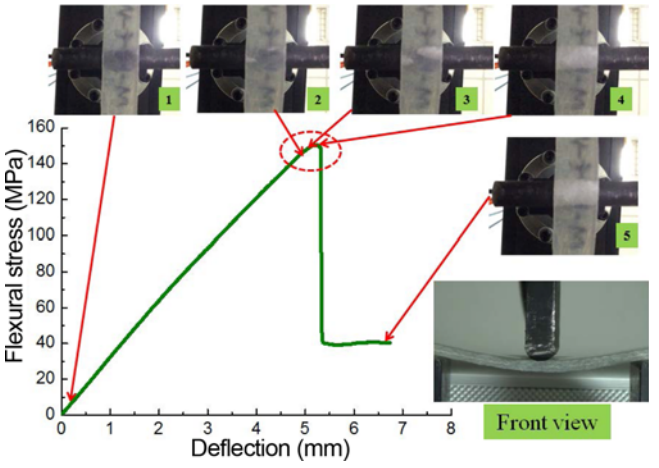

Figure 10. Fracture process in bending test.

The failed specimens were observed under an optical microscope and micrographs were taken in Figures 11 and 12 in order to provide an insight on damage mechanisms. In the case of specimens in the warp direction (i.e. the 0° direction) under flexural loading, it can seen from hybrid composites 3-W had relatively shorter longitudinal crack depth than other two hybrid composites (see Figure 11). The whole crack propagation and delamination were also additionally observed to less serious. With respect to LCBF experiments, take hybrid composites 3-W and GFRP as examples, optical micrographs displayed in Figure 12 that shorter longitudinal crack depth and less serious delamination were found for hybrid composites compared to GFRP.

The common failures under flexural loading includes compressive failure, tensile failure, shear and/or delamination, wherein failure by compression is the most common [25]. The initiation of crack occurred at the outermost tensile side layer that was observed in the fractured surfaces, which absorbed most of the applied load, leading to the crack propagation. Consequently, the failure mechanism was dominated by compressive failure located in the tension side.

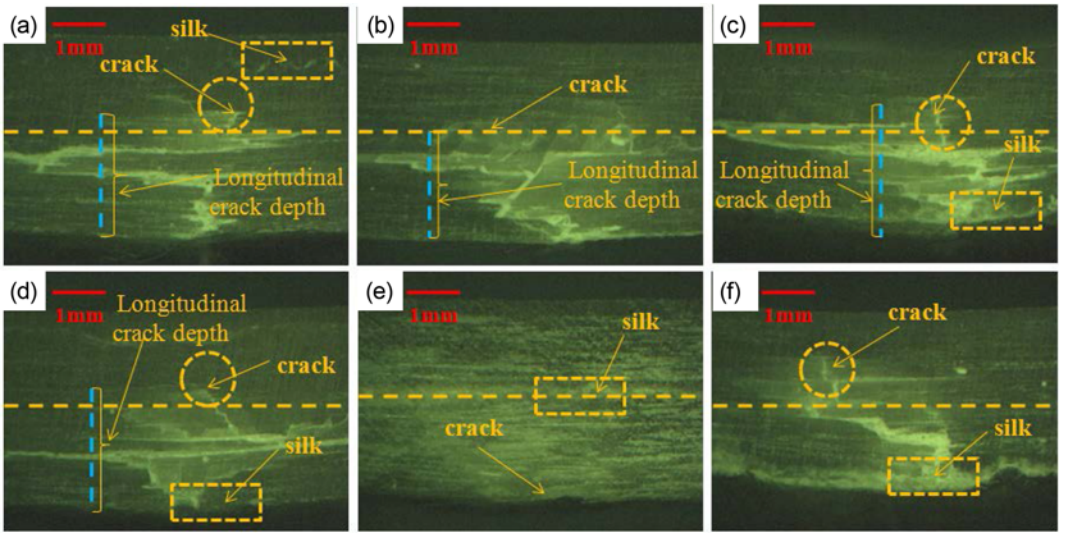

Figure 11. Optical images of failed hybrid composites under flexural loading; (a) 1-W, (b) 3-W, (c) 5-W, (d) 1-F, (e) 3-F, and (f) 5-F.

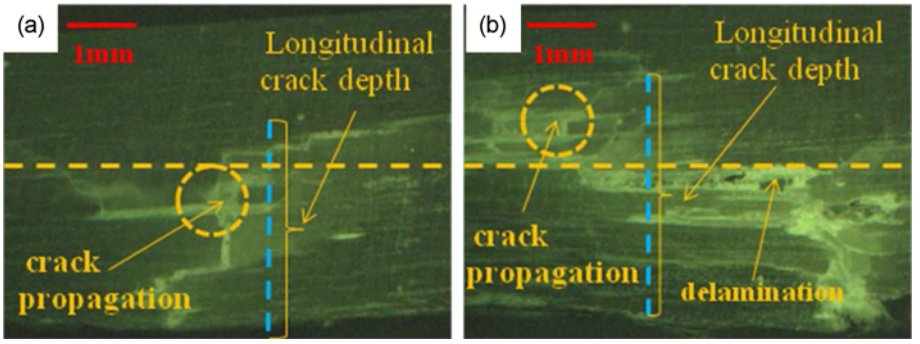

Figure 12. Optical images of failed hybrid composites and GFRP under flexural loading after LCBF test; (a) 3-W and (b) GFRP.

During normal bending and LCBF tests, the top layer of the specimen is subjected to compression, and the bottom layer is subjected to tension. While, the mid-layer is subjected to shear, and hence, the failure of composite is due to a combination of bending and shear. Thus, the effect of compression and tension is relatively weak for mid-layer [26].

It seems that hybrid composites 3-W exhibited better flexural properties than other two hybrid composites. This has been explained with the fact that the mid-layer silk fabric is subjected to lower compression and tension in comparison with first-layer and last-layer silk fabric which leads to higher carrying loading by the mid-layer silk fabric in the matrix under flexural loading conditions, i.e. the glass mat will withstand primary applied flexural load due to higher mechanical properties than natural fibers while mid-layer silk fabric is subjected to lower compression and tension. When GSFRP laminates with mid-layer silk fabric is under applied flexural load, the load is transferred to the silk fibers and the silk fibers are able to carry some of the load since the silk fabric didn't break. Thus, this may result in slowing down the crack propagation process in the hybrid composites. Thus, this may result in slowing down further propagation of the crack and alleviatinge the delamination of the specimens during the bending process. As a result, silk fabric inserted in the middle layer didn't deteriorate the integral flexural performance, or even improved flexural performance. In LCBF test, fatigue stress is effectively distributed in fibers, thus it can withstand more stress leading to higher flexural strength. Thus, inserted silk fabric can hinder the crack damage in the matrix and fibers from propagating leading to higher anti-fatigue property to GFRP specimens.

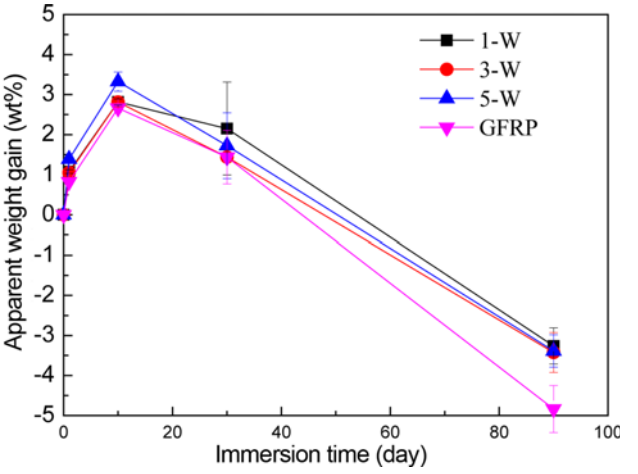

Figure 13. Apparent weight gain.

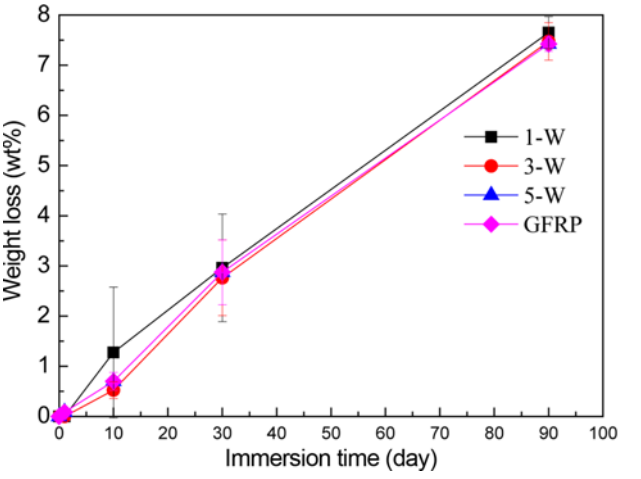

Figure 14. Percentage of weight loss.

Results of Hydrothermal Aging Test

Weight Changes Characteristics

The apparent weight gain (WG) as a function of immersion time for hybrid composites and GFRP are shown in Figure 13. It can be seen that for all the four composites investigated, WG increased monotonically with immersion time initially before reaching a maximum. This is in accord with most moisture absorption studies on GFRP [27]. In addition, the moisture absorption of silk fiber led to higher WA increase of hybrid composites compared with that of GFRP. Approximately, the maximum WG for hybrid composites 1-W, 3-W and 5-W was around 2.8 %, 2.8 % and 3.3 %,

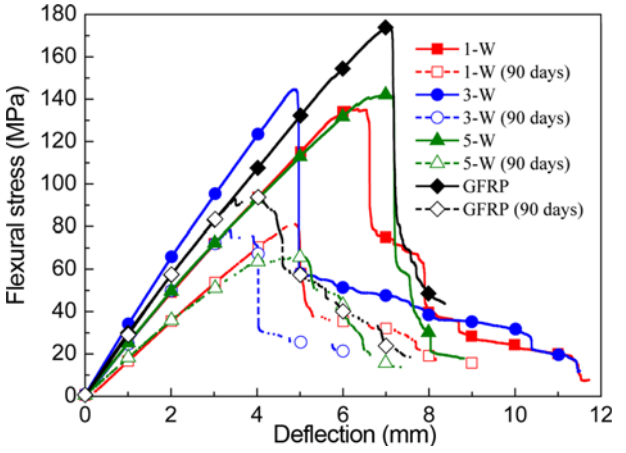

Figure 15. Typical flexural stress-deflection curves in the dry and water treated conditions.

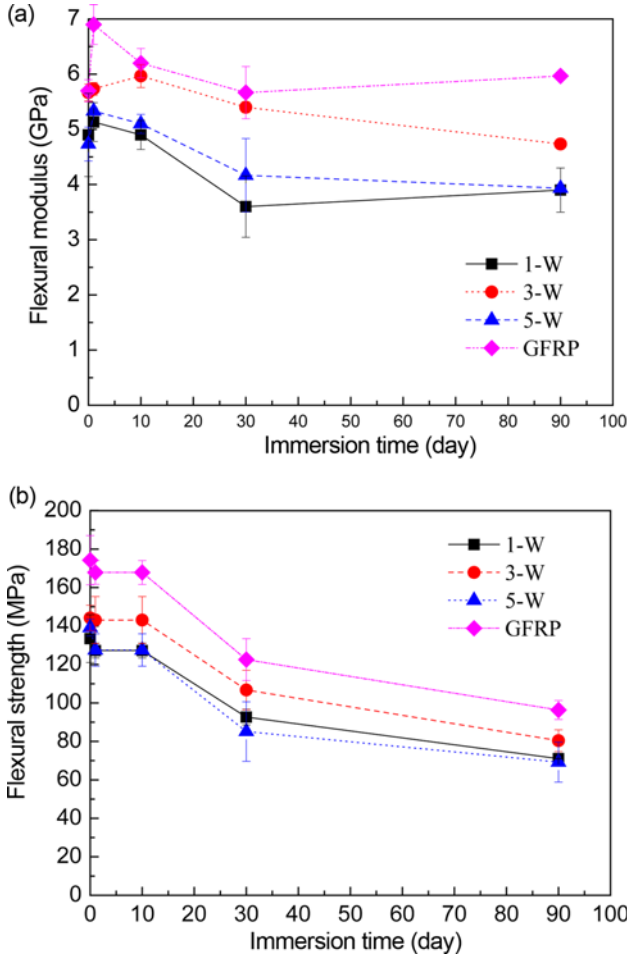

Figure 16. Flexural behavior subjected to different water immersion duration; (a) flexural modulus and (b) flexural strength.

respectively. while it was about 2.7 % for GFRP. When the exposure time was prolonged further after 10 days, the WG

Figure 17. Photos showing the surfaces for hybrid composites 3-W subjected to different water immersion duration; (a) 0 day and (b) 90 days.

was found to decrease after passing through a maximum. After prolonged water immersion treatment for 90 days, the WG for respective composite was around -3.3 %, -3.4 %, -3.4 % and -4.8 %. This is caused by peeling of the neat resin layer and dissolving away of both the neat resin layer and silk fiber with exposure time (see photo of Figure 17(b)).

In order to better understand the moisture absorption characteristics for hybrid composites, the percentage of weight loss (WL), as defined by equation (2), was also measured. The percentage of weight loss (WL) as a function of immersion time for hybrid composites and GFRP are shown in Figure 14. WL increased steadily with the exposure time. At a given water immersion time, it can be seen that WL was more severe for hybrid composites compared with that of GFRP.

Bending Results

Typical flexural stress-deflection curves for hybrid composites and GFRP before (labeled as 0 day) and after water immersion for 90 days are compared in Figure 15. It is obvious that both the stacking sequence and water immersion treatment had an obvious influence on the flexural characteristics for the composites. From flexural stress-deflection curves, flexural modulus, flexural strength of hybrid composites and GFRP are obtained and they are plotted as a function of immersion time in Figure 16(a), (b), respectively. It can be seen from Figure 16(a) and (b) that both flexural modulus and flexural strength were enhanced at the initial stage of water immersion treatment after 1 day degradation compared with non-degraded ones. The initial increase of the mechanical properties has been reported for various FRP systems [28]. However, after prolonged water immersion treatment, both flexural modulus and flexural strength degraded sharply with increase in the water immersion time after 30 days. The retention of flexural strength of hybrid composites 1-W, 3-W, 5-W and GFRP was 53.2 %, 55.8 %, 49.8 %, and 55.3 % after 90 days immersion, respectively. On the contrast, flexural modulus was relatively less deteriorated with the exposure time. The corresponding retention of respective flexural modulus was 79.6 %, 82.5 %, 83.0 % and 98.0 % as the exposure time up to 90 days. Additionally, the retention of flexural properties after aging in respective composite

were also compared. It revealed that hybrid composites 3-W represented an relatively mild deteriorate effect with around 55.8% retention of flexural strength and 82.5 % retention of flexural modulus. The inserted silk fabric hardly enhanced the effect of hydrothermal aging on GFRP specimens.

There are three main mechanisms that can be considered to affect the flexural modulus and flexural strength from water immersion:

(I) The reinforcing effect of glass fiber and silk fiber in unsaturated polymer (UP) matrix and or relaxation of the internal stress formed during fabrication are believed to be responsible for the increase of the flexural properties in the short water treatment duration states [28].

(II) The second is the plasticization effect of the absorbed water molecules so that the interfacial bond strength between glass fiber, silk fiber and the UP matrix has been weakened, leading to reduced flexural properties. This mainly occurs with short immersion duration at the initial stage [29].

(III) The third mechanism is from the weakening of the silk fibers due to the leaching out of the fiber materials and the hydrolysis effect from the water immersion treatment. When the water immersion time exceeded the initial stage, the hydrothermal effect bring in the permanent degradation of the resin system [29]. In addition, both the fiber/matrix interface and the fiber integrity have been severely damaged. As a result, both the stress transfer and load bearing ability of the composites have been degraded.

The photos of hybrid composites 3-W in the dry and water treated for 90 days states are taken by digital camera as presented in Figure 17(a), (b), respectively. Less resin adhered to the fiber can be seen than that of the corresponding unaged material (see photo of Figure 17(a)). This is due to the neat resin layer peeling and dissolving away of the neat resin layer with exposure time.

Izod Impact Results

Absorbed energy of different hybrid composites and GFRP laminates with non-degraded and degraded treatment after pendulum Izod impact are summarized in Figure 18. The Izod impact strength was improved from the water immersion treatment after 1 day degradation initially until reaching a maximum value. Nevertheless, specimens' impact strength presented a monotonically decreasing trend after 30 days degradation, in which 1-W, 3-W, 5-W and GFRP showed the respective decrement of 58.1 %, 52.5 %, 52.1 % and 58.2 % after a prolong period of 90 days water immersion. It can be also seen that the inserted silk fabric hardly aggravated the effect of hydrothermal aging on GFRP specimens for Izod impact properties.

The morphology of GFRP specimens in the dry and water treated for 1day, 90 days states are observed by scanning electron microscopy as presented in Figure 19(a), (b) and (c), respectively. In fact, as documented in Figure 19(b), the interfacial failure after immersion in water for 1 day was less serious, and more resin adhered to the fiber than that of the

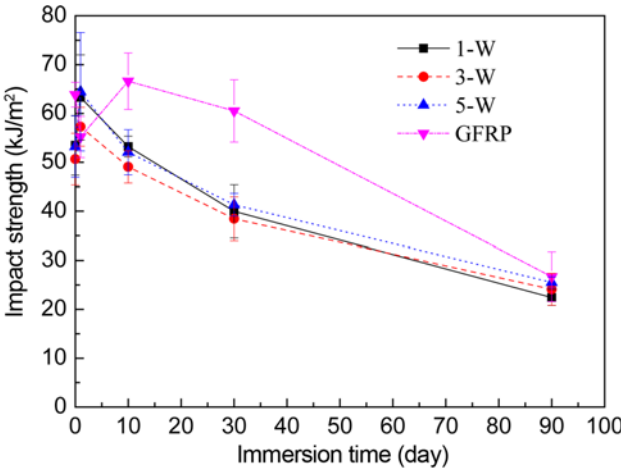

Figure 18. Izod impact strength subjected to different water immersion duration.

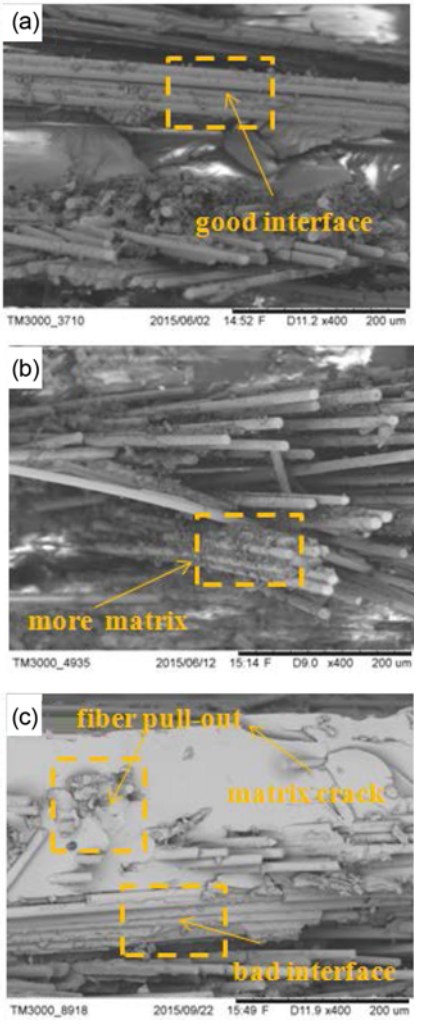

Figure 19. SEM micrographs showing the impact fracture surfaces for GFRP specimens subjected to different water immersion duration; (a) 0 day, (b) 1 day, and (c) 90 days.

corresponding unaged material (see micrograph of Figure 19(a)). The effective stress transfer ability across the fiber/matrix interface resulted in the significant enhancement in the impact strength (Figure 19(b)). For the specimen that has been water treated for 90 days (Figure 19(c)), it is found that the surface of fibers was smooth with a small amount of resin adhered on the surface, meanwhile fiber pull-out, matrix cracking and serious debonding between fiber and matrix can be observed, which was mainly related to fiber/matrix interface failure, resulting in the degradation of impact strength.

The improvement in the impact strength is related to the plasticization effect of the glass fiber/UP and silk fiber/UP interface, which will encourage the fiber pull-out mechanism. On the other hand, a strong fiber/matrix interface is beneficial to the flexural strength, while it has a detrimental effect on the impact strength as energy absorption from the fiber/matrix debonding and fiber pullout will be suppressed [30]. Additionally, there will be some swelling of the silk fiber diameter with the absorption of a small amount of moisture. The swelling of the silk fibers will enhance the frictional work from fiber pullout performance from the UP matrix [31]. However, On extending a period of water treatment, excess swelling with extraction of the water soluble substances from the silk fibers will cause damage to the fiber structure. The damages in the fiber structure will provide additional channels for water to diffuse into the hybrid composites and lead to further weakening the fiber/matrix interface. At this stage, the impact strength for the hybrid composites will degrade with further increase in the water exposure time.

Impact fracture surface morphologies for hybrid specimens 3-W subjected to different extent of water immersion are displayed in Figure 20. The fracture surface for a dry sample is illustrated in Figure 20(a), the surface of the pullout silk fiber was covered with a thick layer of matirx, and indicated cohesive failure. For the specimen that has been water treated for 1 day (Figure 20(b)), it can be seen that the silk fiber was still a relatively intact fiber, whose surface was covered with maxtrix. With the water immersion treatment extended to 30 days (Figure 20(c)), the interface between fiber and matrix can be seen to be severely damaged. The impact strength of the composite at this state had already decreased. On extending the water immersion to 90 days, it can be seen from Figure 20(d) that on top of the deteriorated fiber/matrix interface, the layer of some substances on the silk fiber surface had been dissolved as well. The scanning electron micrograph (Figure 20(b) and 20(c)) reveals the fibre pull out from the matrix, poor interface between fiber and matrix, indication poor adhesion between the reinforcement and the matrix. With the water immersion treatment extended further, fiber-matrix debonding, matrix crack and fibre pull out is more evident in hybrid composites.

Conclusion

This study explored the possibility of incorporating silk

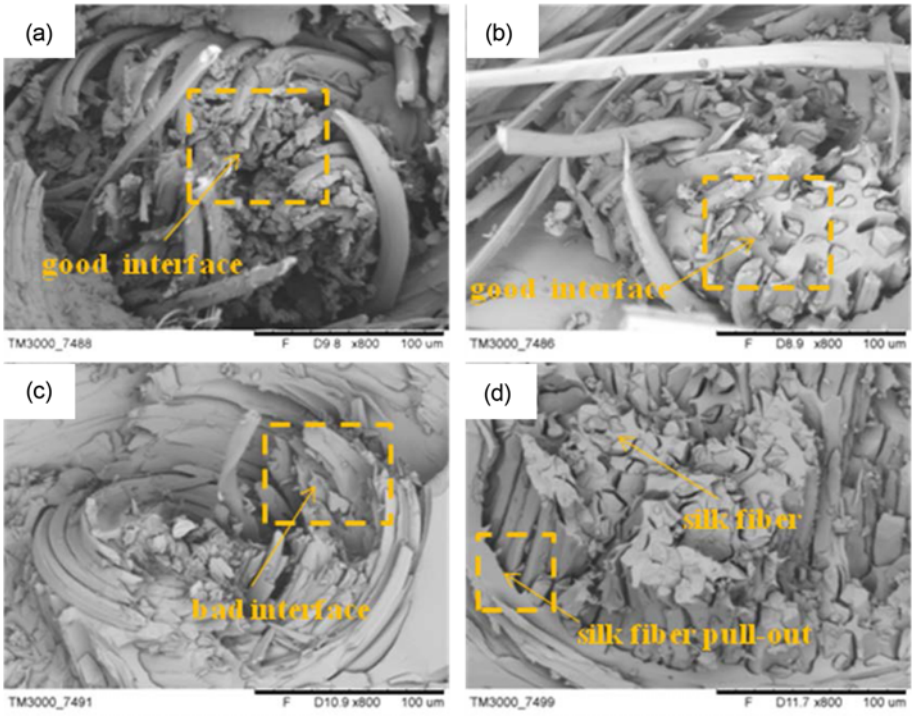

Figure 20. SEM micrographs showing the impact fracture surfaces for 3-W specimens subjected to different water immersion duration; (a) 0 day, (b) 1 day, (c) 30 days, and (d) 90 days.

fabric into glass mat reinforced composites and investigated the effect of stacking sequence on the flexural properties (i.e. three-bending and LCBF properties) of hybrid composites. In addition, the effects of water immersion treatment (at 80 °C) on the bending and impact behaviors have also been investigated. The following points are drawn from the experimental results:

1. The stacking sequence was found to affect the flexural properties of the hybrid composites. Higher flexural modulus and strength were achieved when silk fabric layer was stacked at the middle layer, with 3-W (i.e., stacking respective two glass mat layer at the tension side and compressive side) showing the best flexural strength and modulus that exhibited about respective 16.3 % and 8.1 % higher than the values of 1-W from among the stacking sequence arrangements. In addition, the minimum flexural deflection obtained for 3-W was approximately 16.1 % below than that of 1-W. This has been explained with the fact that the middle-layer silk fabric is subjected to lower compression and tension in comparison to first-layer and last-layer silk fabric which leads to the higher carrying loading by the middle-layer silk fabric in the matrix during loading conditions, i.e. the glass mat will withstand primary applied flexural load due to higher mechanical properties than natural fibers while mid-layer silk fabric is subjected to lower compression and tension. When GSFRP laminates with mid-layer silk fabric is under applied flexural load, the load is transferred to the silk fibers and the silk fibers are able to carry some of the load since the silk fabric didn't break. Thus, this may enhance the ability of preventing the propagation of crack in the hybrid composites. The bending results showed that the dominant failure mode was compressive failure. In fact, GFRP showed higher flexural properties than 3-W due to high fiber content.
2. Investigations on LCBF behavior revealed that for hybrid composites and GFRP, flexural modulus did not vary much during the LCBF test. Flexural strength of GFRP specimens changed when the pre-set load was enhanced to 85 %. While it hardly changed for hybrid composites even though the pre-set load was up to 85 %. The addition of silk fabric in the hybrid composites may result in slowing down the crack propagation process. Fatigue stress is effectively distributed in fibers, thus it can withstand more stress leading to higher flexural strength. Therefore, the anti-fatigue property has been improved by the inclusion of silk fabric reinforced in glass mat hybrid composites.
3. Flexural properties of hybrid composites in the 0 ° and 90 ° directions showed no much variation in the three-point flexural quasi-static and load-controlled low cycle bending fatigue (LCBF) tests.
4. From the apparent weight gain (WG) measurement, it is observed that the value of WG increased monotonically with immersion time before reaching a maximum and then decreased after passing through water immersion treatment for 10 days. With respect to weight loss (WL), it is found to increase sharply with increasing immersion time. In the water immersion experiments, both the flexural properties and impact properties were improved initially until reaching the maximum and then decreased continuously with extending the water immersion time. These seemingly contradictory behaviours are due to relaxation of the internal stress, swelling of the silk fibers and the weakening of fiber/matrix interface. Nevertheless, the inserted silk fabric hardly aggravated the effect of hydrothermal aging on GFRP specimens.

Acknowledgements

The author Zhao defang is grateful to Group students Dong yuying, Hu peng and Xu jing for their help with experiments and to professors Yang yuqiu and Hiroyuki Hamada for discussions throughout the work. Laminates were produced at Mazda Motor Corporation whose cooperation is invaluable. The author also expresses his gratitude to Erika Suzuki, Yuka Takai and Takashi Furukawa for their support and technical collaboration.

References

1. A. F. Hamed, M. M. Hamdan, and B. B. Sahari, *ARPN J. Eng. Appl. Sci.,* **3**, 76 (2008).
2. J. G. Morley, "High Performance Fiber Composites", pp.125-167, Academic Press, Orlando, 1987.
3. G. Belingardi, M. P. Cavatorta, and C. Frasca, *Compos. Sci. Technol.*, **66**, 222 (2006).
4. N. Kulkarni, H. Mahfuz, and S. Jeelani, *Compos. Struct.*, **59**, 499 (2003).
5. R. A. A. Couillard and P. Schwartz, *Compos. Sci. Technol.*, **57**, 229 (1997).
6. Z. Xu, B. Xiao, and T. Hojo, *J. Biobased Mater. Bioenergy*, **9**, 188 (2015).
7. O. J. Nixon-Pearson, S. R. Hallett, and P. J. Withers, *Compos. Struct.*, **106**, 882 (2013).
8. O. J. Nixon-Pearson, S. R. Hallett, and P. W. Harper, *Compos. Struct.*, **106**, 890 (2013).
9. E. G. Koricho, G. Belingardi, and A. T. Beyene, *Compos. Struct.*, **111**, 169 (2014).
10. W. Van Paepegem and J. Degrieck, *Compos. Struct.*, **51**, 1 (2001).
11. P. Purnell, J. Cain, P. V. Itterbeeck, and Lesko, *Compos. Sci. Technol.*, **68**, 3330 (2008).
12. J. Jedidi, F. Jacquemin, and A. Vautrin, *Compos. Pt. A-Appl. Sci. Manuf.*, **37**, 636 (2006).
13. T. Alfrey, E. F. Gurnee, and W. G. Lloyd, *J. Polym. Sci. Pt. C*, **12**, 249 (1966).
14. P. Nogueira, C. Ramírez, A. Torres, M. J. Abad, J. Cano,

and J. López, *J. Appl. Polym. Sci.*, **80**, 71 (2001).
15. O. Starkova, S. T. Buschhorn, E. Mannov, K. Schulte, and A. Aniskevich, *Eur. Polym. J.,* **49**, 2138 (2013).
16. C. J. Tsenoglu, S. Pavlidou, and C. D. Papaspyrides, *Compos. Sci. Technol.*, **66**, 2855 (2006).
17. M. L. Costa, M. C. Rezende, and S. F. M. De Almeida, *J. Compos. Mater.,* **39**, 1943 (2005).
18. A. Y. Zhang, D. H. Li, D. X. Zhang, H. B. Lu, H. Y. Xiao, and J. Jia, *Express Polym. Lett.*, **5**, 708 (2011).
19. J. Zhou and J. P. Lucas, *Compos. Sci. Technol.*, **53**, 57 (1995).
20. Y. Yang, T. Ota, T. Morii, *J. Mater. Sci.*, **46**, 2678 (2011).
21. M. Liao, Y. Yang, and Y. Yu, *Proc. ASME 2012 Inter. Mech. Eng. Cong. Expo.*, **3**, 1371 (2012).
22. K. Hamano, Y. Yang, and Z. Zhang, *Proc. ASME 2012 Inter. Mech. Eng. Cong. Expo*, **3**, 1225 (2012).
23. Y. Yu, Y. Yang, and K. Tanabe, *J. Biob. Mater. Bioe.*, **5**, 117 (2011).
24. D. R. Moore, J. G. Williams, and A. Pavan, "Fracture Mechanics Testing Methods for Polymers, Adhesives and Composites", p.396, Elsevier, New York, 2001.
25. C. S. Dong, H. A. Ranaweera-Jayawardena, and I. J. Davies, *Compos. Pt. B-Eng.*, **43**, 573 (2012).
26. R. Vinayagamoorthy and N. Rajeswari, *J. Reinf. Plast. Comp.*, **33**, 81 (2014).
27. M. A. G. Silva, *Compos. Struct.*, **79**, 97 (2007).
28. G. Xian, H. Li, and X. Su, *Polym. Compos.*, **33**, 1120 (2012).
29. I. Ghorbel and D. Valentin, *Polym. Compos.*, **14**, 324 (1993).
30. K. L. Fung, R. K. Y. Li, and S. C. Tjong, *J. Appl. Polym. Sci.*, **85**, 169 (2002).
31. C. P. L. Chow, X. S. Xing, and R. K. Y. Li, *Compos. Sci. Technol.*, **67**, 306 (2007).